Am J Physiol Heart Circ Physiol 309: H1130–H1140, 2015.
First published August 7, 2015; doi:10.1152/ajpheart.00123.2014.

Alagebrium inhibits neointimal hyperplasia and restores distributions of wall shear stress by reducing downstream vascular resistance in obese and diabetic rats

Hongfeng Wang,[1] Dorothee Weihrauch,[2] Judy R. Kersten,[2] Jeffrey M. Toth,[1,3] Anthony G. Passerini,[4] Anita Rajamani,[4] Sonja Schrepfer,[5,6] and John F. LaDisa, Jr.[1,7,8]

[1]*Department of Biomedical Engineering, Marquette University, Milwaukee, Wisconsin;* [2]*Department of Anesthesiology, Medical College of Wisconsin, Milwaukee, Wisconsin;* [3]*Department of Orthopaedic Surgery, Medical College of Wisconsin, Milwaukee, Wisconsin;* [4]*Department of Biomedical Engineering, University of California Davis, Davis, California;* [5]*Transplant and Stem Cell Immunobiology Laboratory, University Heart Center and Cardiovascular Research Center, University of Hamburg, Hamburg, Germany;* [6]*Department of Cardiothoracic Surgery, Stanford University School of Medicine, Stanford, California;* [7]*Department of Medicine, Division of Cardiovascular Medicine, Medical College of Wisconsin, Milwaukee, Wisconsin;* [8]*Biotechnology and Bioengineering Center, Medical College of Wisconsin, Milwaukee, Wisconsin*

Submitted 20 February 2014; accepted in final form 3 August 2015

Wang H, Weihrauch D, Kersten JR, Toth JM, Passerini AG, Rajamani A, Schrepfer S, LaDisa JF Jr. Alagebrium inhibits neointimal hyperplasia and restores distributions of wall shear stress by reducing downstream vascular resistance in obese and diabetic rats. *Am J Physiol Heart Circ Physiol* 309: H1130–H1140, 2015. First published August 7, 2015; doi:10.1152/ajpheart.00123.2014.—Mechanisms of restenosis in type 2 diabetes mellitus (T2DM) are incompletely elucidated, but advanced glycation end-product (AGE)-induced vascular remodeling likely contributes. We tested the hypothesis that AGE-related collagen cross-linking (ARCC) leads to increased downstream vascular resistance and altered in-stent hemodynamics, thereby promoting neointimal hyperplasia (NH) in T2DM. We proposed that decreasing ARCC with ALT-711 (Alagebrium) would mitigate this response. Abdominal aortic stents were implanted in Zucker lean (ZL), obese (ZO), and diabetic (ZD) rats. Blood flow, vessel diameter, and wall shear stress (WSS) were calculated after 21 days, and NH was quantified. Arterial segments (aorta, carotid, iliac, femoral, and arterioles) were harvested to detect ARCC and protein expression, including transforming growth factor-β (TGF-β) and receptor for AGEs (RAGE). Downstream resistance was elevated (60%), whereas flow and WSS were significantly decreased (44% and 56%) in ZD vs. ZL rats. NH was increased in ZO but not ZD rats. ALT-711 reduced ARCC and resistance (46%) in ZD rats while decreasing NH and producing similar in-stent WSS across groups. No consistent differences in RAGE or TGF-β expression were observed in arterial segments. ALT-711 modified lectin-type oxidized LDL receptor 1 but not RAGE expression by cells on decellularized matrices. In conclusion, ALT-711 decreased ARCC, increased in-stent flow rate, and reduced NH in ZO and ZD rats through RAGE-independent pathways. The study supports an important role for AGE-induced remodeling within and downstream of stent implantation to promote enhanced NH in T2DM.

coronary artery disease; hemodynamics; hyperglycemia; interventional cardiology; restenosis

NEW & NOTEWORTHY

Alagebrium (ALT-711) decreased advanced glycation end-product–related collagen cross-linking and arteriolar stiffness in stented obese and diabetic rats, resulting in decreased downstream resistance and increased in-stent blood flow and wall shear stress. ALT-711 was effective at reducing neointimal hyperplasia and promoting endothelial proliferation regardless of glycemic status.

IT IS ESTIMATED THAT 25.8 MILLION Americans are diabetic (8.3% of the population), and an additional 79 million have the metabolic syndrome, a constellation of clinical findings that substantially increases the risk for developing type 2 diabetes mellitus (T2DM) (7). Cardiovascular disease (CVD) accounts for 68% of diabetes-related deaths among people aged 65 yr or older, as these patients have a two- to fourfold increased risk of developing coronary and peripheral artery disease (7, 19).

Bare-metal stents (BMS) can restore blood flow (BF) beyond a vascular occlusion, but restenosis occurring primarily as a result of excessive neointimal hyperplasia (NH) limits their success. These cases require revascularization of the restenotic lesion and have cost the U.S. healthcare system more than $2.5 billion since 1999 (40). Drug-eluting stents (DES) have also been used to combat CVD but are less effective for patients with T2DM (18, 32). Sirolimus and paclitaxel (antiproliferative agents) used with early-generation DES impede healing of the intima after implantation, thereby inhibiting coverage of the stent linkages by endothelial cells (ECs) and making the vessel more prone to late thrombosis (20, 22). Newer generation DES with zotarolimus and everolimus more favorably inhibit the proliferation of smooth muscle cells (SMC) and inflammatory cells (26), but improvements in mortality, myocardial infarction, stent thrombosis, and target lesion revascularization afforded to patients with normoglycemia with these newer DES have not translated to patients with diabetes (11, 44).

Mechanisms for the elevated restenosis rates after stenting in patients with T2DM compared with normoglycemia have not yet been fully elucidated. It has been suggested that the current paradigm concerning the use of stents in patients with T2DM applies methods from retrospective revascularization studies conducted in patients with normoglycemia to T2DM in hopes that poor outcomes do not occur (3). In contrast, some investigators have examined pharmacological agents such as antisense oligonucleotides and L-arginine supplementation to im-

Address for reprint requests and other correspondence: J. LaDisa, Jr., 1637 West Wisconsin Ave., Milwaukee, WI 53233 (e-mail: john.ladisa@marquette.edu).

prove endothelial function, but these pharmacological agents failed to alleviate restenosis in T2DM (15, 27).

Although local changes in cytokine release and cell signaling undoubtedly play a role in this process, the inciting changes in local and distal fluid dynamics and vascular biomechanics associated with T2DM, which may also contribute to restenosis, have been relatively ignored. For example, adverse structural modifications are known to occur throughout the arterial system in response to T2DM, including increased vascular stiffness attributable to advanced glycation end-products (AGEs), which are formed through nonenzymatic reaction between glucose and proteins. It has been reported that AGEs can cause tissue damage in the cardiovascular system by cross-linking with collagen, thus disrupting the vessel wall and altering compliance (i.e., increasing stiffness) (39). These changes may be manifested by an increase in vascular resistance (DVR) at the arterioles that may have an important impact within the upstream stented region in terms of local flow patterns, blood pressure (BP), and altered wall shear stress (WSS) that have previously been correlated with NH (29).

AGEs, which form more rapidly during diabetes as a consequence of chronic hyperglycemia (38, 49), also play an important role in cell signaling to influence NH. For example, they may react with a receptor (RAGE) to increase oxidative stress, expression of transforming growth factor-β (TGF-β), and extracellular matrix accumulation (35).

Alagebrium (ALT-711; 3-phenacyl-4, 5-dimethylthiazolium chloride) has been shown to cleave AGE-related collagen cross-linking (ARCC), thereby decreasing vessel resistance and atherosclerosis (2, 10). ALT-711 may consequently further decrease NH in T2DM by modulating in-stent hemodynamics secondary to its effects on downstream resistance vessels. Therefore, we tested the hypothesis that ARCC leads to increased DVR and altered hemodynamics in the stented region, promoting enhanced NH after BMS implantation in T2DM. We further proposed that that decreasing ARCC with ALT-711 would mitigate this response.

MATERIALS AND METHODS

In vivo protocol. Stents were deployed into the abdominal aorta (AAo) of male Zucker lean (ZL), obese (ZO), and diabetic (ZD) rats ($n = 9$/group) in the absence or presence of ALT-711 (i.e., treatment). After 21 days, three rats from each group were randomly selected for AAo casting and measurement of local BF and vessel diameter to calculate in-stent WSS. Remaining rats underwent quantification of NH, ARCC, and protein expression by Western blotting. Additional details are provided below.

In vivo experimental preparation. All procedures were approved by the Animal Care and Use Committees of the Medical College of Wisconsin and Marquette University and conformed to the *Guide for the Care and Use of Laboratory Animals* published by the U.S. National Institutes of Health. ZL, ZO, and ZD rats (Charles River Laboratories, Wilmington, MA) were selected randomly for stenting at 12 wk of age after >48 h of acclimation. Rats were anesthetized in an induction chamber using 1–2% isoflurane then placed on a warm surface and fitted with a nose cone attached to an anesthetic vaporizer to maintain the proper plane of anesthesia (~0.5–3.0%).

Stent implantation in vivo. AAo stenting was performed under anesthesia and sterile conditions (12, 36). Local BF patterns and the subsequent severity of NH are influenced by stent geometry (29). Stainless steel balloon expandable stents (316L) specially designed for the rat AAo (2.5 × 8 mm) and with a known geometric pattern were therefore purchased from Burpee Materials Technology (Eatontown, NJ) and crimped on 2.5 × 12 mm rapid-exchange delivery catheters (Polymerex, San Diego, CA). In preparation for stenting, the site above the AAo and iliac arteries was shaved and cleaned. The skin was then incised by a midsagittal incision. Under microscopic view, the AAo and iliac arteries were carefully separated free from surrounding vessels and tissue. Small aortic side branches were temporarily clamped to limit the backflow of blood. Vascular clips were placed to isolate the region undergoing stenting near the aorta-iliac bifurcation. A small incision was made in the isolated segment, and blood was removed by rinsing with heparinized saline (100 U/kg) to prevent acute thrombosis. The tip of a delivery catheter and guide wire were then inserted. Clamps were then briefly removed as necessary to thread the stent to an infrarenal segment of the AAo. The stent was then inflated to securely anchor it against the AAo wall using 10–20% overexpansion (17). Successful deployment was confirmed visually through the AAo wall. After removal of the stent delivery catheter, the incision was closed using an 8-0 suture. The vascular clips were then removed, and the abdomen was closed with 4-0 silk suture while the skin was closed with 4-0 dissolvable Vicryl suture using stitches just below the skin.

Surgical and postoperative care. Quantitative criteria including oxygen saturation, respiration, temperature, pulse, mucous membrane color, and capillary refill time were continuously monitored during the surgical procedure and 3–4 h after its completion. Buprenorphine (0.05 mg/kg ip) was used as analgesia for 2 days. Animals also received antibiotic prophylaxis (20 mg/kg cefazolin ip) for 4 days and aspirin in their food or drinking water (20 mg/day) for the duration of the experiment to prevent thrombosis.

ALT-711 treatment in vivo. An inhibitor of ARCC, ALT-711 (Iron-Dragon, Newport Beach, CA) was delivered at a dose of 1.0 mg/kg per day for 21 days using an osmotic minipump (ALZET, Cupertino, CA) to avoid daily injections. Before skin was closed after stenting, a minipump was filled, placed just beneath the muscle layer, and positioned with its delivery portal facing cranially. All other procedures were equivalent, and four additional ZL rats underwent stenting and minipump insertion with vehicle alone (i.e., saline).

Hemodynamic data acquisition. Rats were anesthetized 21 days after stenting as described above, and the right carotid artery was isolated. A fluid-filled catheter connected to a BP transducer (Harvard Apparatus, Holliston, MA) was calibrated and inserted from the carotid artery into the aorta. The AAo proximal to the stent was also dissected free from connective tissue and the vena cava, so BF could be recorded with a transit-time flow probe connected to a flow meter (Transonic Systems, Ithaca, NY). BP and BF data were sampled using an A/D converter interfacing with a laptop running WINDAQ software (DATAQ Instruments, Akron, OH). Rats were then euthanized by overdose pentobarbital sodium (100 mg/kg iv).

Calculation of in-stent WSS. The stented region was carefully dissected from connective tissue after euthanasia. A small incision was made in the suprarenal AAo, and a catheter containing Batson's No. 17 Corrosion Compound (Polysciences, Warrington, PA) was secured within the vessel (29). A four-way stopcock was connected to the catheter and BP transducer. A syringe was then connected to the open end of the stopcock to flush the vessel with saline before the plastic compound was injected and maintained at the mean BP measured for each rat. Care was taken to ensure no bubbles were injected, and mean BP was maintained, thereby capturing the geometry of the flow domain. After curing (2–3 h), surrounding tissue was caustically removed with Batson's No. 17 Maceration Solution, leaving a cast of the flow domain. In-stent WSS was calculated as $4\mu Q/\pi r^3$, where Q is the mean measured flow rate, viscosity was assumed to be 6.2 cP (53), and r is the radius determined from an average of three digital micrometer measurements within the stented region.

Quantification of NH. The stented AAo of rats not undergoing casting was rinsed with saline to remove any blood and fixed in 4% paraformaldehyde for >24 h. Vessels were then dehydrated in 70%

ethanol for 2 h, 95% ethanol for 2 h, and 100% ethanol twice for 2 h. Following dehydration, samples underwent preinfiltration for 2 h and infiltration for 24 h. Samples were then embedded in glycol methacrylate (EB Sciences, Agawam, MA), sectioned at room temperature in 5-μm intervals using a microtome equipped with a tungsten carbide blade (Ted Pella, Redding, CA), and stained with hematoxylin and eosin (H and E). Briefly, plastic stent sections were stained by Gill's hematoxylin for 15 min followed by three distilled water washes. Scott's tap water was used for 2 min followed by an additional three washes with distilled water. Sections were then counterstained with eosin for 5 min, dehydrated carefully using 96% and 100% ethanol, cleared in xylene, and mounted with a xylene-based mounting medium. Images were obtained using a Zeiss Universal microscope with ×2.5 and ×4 objective lenses coupled to a 16-bit Leica DFC 280 digital camera using Image Pro Plus 5.1 image analysis software running on a Windows XP workstation. NH was quantified from the middle of the stented region to avoid contributions resulting from flow disturbances or pronounced vessel injury. The percentage of vascular lumen in which NH occurred was quantified by subtracting the luminal area from that bounded by the stent with NIH ImageJ software (29).

Analysis of ARCC and protein expression. Vessels from elastic arteries (aorta and carotid arteries), peripheral muscular arteries (femoral and iliac arteries), and smallest distal arteries (cremaster arterioles) were harvested. Portions of these vessels from six rats before and after ALT-711 treatment were separately allocated for ARCC or protein analysis. All vessels were snap frozen in liquid nitrogen and stored at −80°C to avoid protein degradation after rinsing with 4°C saline to remove any blood.

Vessel segments analyzed for ARCC underwent pepsin digestion (43). Briefly, vessel segments were lyophilized for >8 h to obtain their dry weight. Dry samples (10 mg) were then treated with 4 mol/l guanidine-HCL in 0.05 mol/l sodium acetate (pH 5.8) at 4°C for 24 h to remove proteoglycans. After centrifugation for 30 min at 30,000 *g*, the residue was collected and washed three times using 0.5 mol/l acetic acid. The collagen residue was added to a solution of 1 mg/ml pepsin in 0.5 mol/l acetic acid at 4°C for 3 days, and undigested material was discarded by centrifugation for 20 min. AGE-related fluorescence of the supernatant was measured by 365-nm excitation and 418-nm emission before being reacted with Sirius red in 0.5 mol/l acetic acid and incubated at room temperature for 20 min. Samples were then centrifuged at 2,500 *g* for 10 min, and the absorbance of the supernatant was read at 540 nm against a 0.5 mol/l acetic acid blank. A series dilution of collagen I (Life Technologies, Grand Island, NY) was then used to generate a standard concentration and absorbance curve. Previous studies found a linear relationship between Sirius red and optical density and that a 0.5 μmol/l concentration was suitable for collagen quantification without saturation (45). The results are presented as AGE-related fluorescence divided by collagen concentration.

Protein for Western blotting analysis was isolated as previously described (48) and quantified using a spectrophotometer (Beckman Coulter, Brea, CA) with the Bradford method and bovine serum albumin as a standard (4). After stabilization on ice for 30 min, 30 μg of the protein was added to the same amount of Laemmli buffer and incubated in a thermomixer (Eppendorf, Hauppauge, NY) for 5 min at 97°C. The treated protein mix was then loaded into a 4–20% polyacrylamide gel (Criterion; Bio-Rad, Hercules, CA). The gel was run for 10 min at 100 V followed by 50 min at 150 V, and transfer occurred at 100 V for 1 h. The polyvinylidene fluoride membrane was then blocked for 1 h at room temperature. The membrane was reacted with primary antibodies (Table 1) overnight and then secondary antibodies (Table 1) for 1 h at room temperature. The membrane was washed, incubated in enhanced chemiluminescence solution for 5 min, and developed using a molecular imager (Bio-Rad).

Statistical procedures for analysis of in vivo data. Statistical analysis was conducted using multiple ANOVA followed by Tukey-Kramer and post hoc analysis. Changes within and between groups were considered statistically significant when $P < 0.05$, and all data were expressed as means ± SE.

In vitro cell culture and treatment protocols. To elucidate the potential contribution of ARCC to NH, the AAo of additional groups of ZL, ZO, and ZD rats in the absence or presence of ALT-711 treatment ($n = 3$/group; 6 groups) was harvested as described above. The extracellular matrix was then isolated by incubating and agitating in 1% SDS for 12 h at room temperature to dissolve cells. The next day, a Triton X-100 wash (30 min) was performed followed by a thorough PBS rinse (15 min). The isolated matrix was then snap frozen and pulverized with mortar and pestle. The powdered matrix was suspended in Dulbecco's PBS and sonicated on ice for 30 s. Human aortic ECs (HAECs) and umbilical vein ECs (HUVECs) were prepared and maintained in endothelial growth medium-2 with 2% FBS and 1× antibiotic-antimycotic solution before being seeded on the decellularized matrices for experiments at *passages 5–7*. The choice of cell type was selected based on their successful use in prior shearing (HAECs) and static (HUVECs) investigations as discussed below.

Cell-shearing experiments. Hydrodynamic experiments were performed on HAEC monolayers using a microfluidic flow chamber device based on Hele-Shaw stagnation flow theory (14, 46). The device induces a linearly decreasing WSS profile along the center line of the longitudinal axis for a given flow rate when vacuum adhered to a cell monolayer, facilitating the study of a wide range in WSS magnitudes within a single cell monolayer, while preserving information related to the spatial heterogeneity of response. The flow rate was chosen to deliver WSS magnitudes ranging from ~0–16 dynes/cm^2, which captures a range of values experienced in the intrastrut region of an implanted stent within a single experiment.

HAECs were seeded on decellularized matrices derived from the AAo of ZD, ZL, and ZO rats with or without ALT-711 (20 μg/ml in Dulbecco's PBS with 1× antibiotic-antimycotic). Collagen I-coated (100 μg/ml; Invitrogen, Carlsbad, CA) tissue culture substrates were used as a control. Experiments were performed when cells reached 80–90% confluence. Flow chambers were sealed to the HAEC monolayers via a vacuum network. Flow was driven by a Masterflex L/S peristaltic pump (Cole-Parmer, Vernon Hills, IL) in a humidified chamber heated to 37°C for 4 h. Leibovitz-15 medium (GIBCO, Carlsbad, CA), supplemented with 10% FBS, endothelial BulletKit (Lonza, Walkersville, MD), and 1× antibiotic-antimycotic solution, was used as the flow medium to maintain pH in the absence of CO_2.

Immunofluorescence staining of sheared cells. Sheared cells were rinsed with PBS and fixed in 4% paraformaldehyde (Electron Microscopy Sciences, Hatfield, PA) for RAGE analysis. Samples were blocked in 20% donkey serum (Invitrogen) and 1% human serum albumin (CSL Behring, King of Prussia, PA) and incubated with

Table 1. *Antibodies used for WB or IF*

Antibody	Company	Catalog No.	Host	Primary Antibody	Secondary Antibody
AGEs	Abcam	ab23722	Rabbit	1:500	1:2,000
RAGE	Santa Cruz Biotechnology	sc-8230	Goat	1:300 (WB) 1:100 (IF)	1:2,000 1:400
TGF-β	Santa Cruz Biotechnology	sc-146	Rabbit	1:400	1:2,000
β-Tubulin	Abcam	ab6046	Rabbit	1:5,000	1:10,000

β-Tubulin was used as loading control for Western blot (WB). IF, immunofluorescence; AGES, advanced glycation end-products; RAGE, receptor for AGEs; TGF-β, transforming growth factor-β.

Table 2. *Rat weights and hemodynamics in the absence or presence of ALT-711*

	Weight, g		Glucose, mg/dl		HR, beats/min		Mean BP, mmHg	
	−	+	−	+	−	+	−	+
ZL	396 ± 13	378 ± 13	232 ± 18	171 ± 19	263 ± 13	236 ± 5	100 ± 3	92 ± 5
ZO	372 ± 12	416 ± 12	359 ± 19*	276 ± 25*	232 ± 10	235 ± 12	96 ± 4	100 ± 6
ZD	398 ± 11	423 ± 10	428 ± 24*	342 ± 18*	250 ± 10	230 ± 7	97 ± 1	94 ± 6

Values are means ± SE; $n = 6$; significance when $P < 0.05$; *significantly different from Zucker lean (ZL) rats. ZO, Zucker obese rats; ZD, Zucker diabetic rats; HR, heart rate; BP, blood pressure.

polyclonal goat anti-RAGE (Santa Cruz Biotechnology, Santa Cruz, CA) at a concentration of 2 μg/ml, for 2 h. Samples were then incubated with secondary Alexa Fluor-546 (Life Technology) rabbit anti-goat (1:400) for 1 h. Coverslips were mounted using VECTASHIELD mounting medium with DAPI (Vector Laboratories, Burlingame, CA). Representative images were taken at ×40 magnification at each WSS magnitude, corresponding to fixed axial position within the chamber. Images were quantified using ImageJ software. The local background-subtracted mean fluorescence intensity was calculated for each cell (~20–40 over 5 representative images) and averaged for a given WSS for each shear experiment ($n = 3$–4).

EC and SMC proliferation assay. HUVECs and aortic SMCs were similarly cultured on decellularized matrices from the AAo of ZD, ZL, and ZO rats with or without ALT-711 for 72 h using 24-well plates (Fisher Scientific, Waltham, MA) in endothelial growth medium complete media (Lonza) and SMC media (Lonza). After 24 h, cells were trypsinized, and the number of cells was determined with a hemacytometer.

Statistical procedures for analysis of in vitro data. Data were analyzed using Minitab 17 Statistical software. Data were tested for normality using the Kolmogorov-Smirnov test. Differences in RAGE expression over multiple shear conditions for a given matrix were assessed using repeated-measures ANOVA, followed by a Dunnett's post hoc test, comparing each group to the static (0 dynes/cm^2) condition. Differences between two groups were assessed using Student's *t*-test. Two-tailed *P* values of <0.05 were considered statistically significant.

RESULTS

Body weight, heart rate (HR), and mean BP were similar in ZL, ZO, and ZD groups in the absence or presence of ALT-711. Implantation of osmotic pumps with saline alone did not affect blood glucose concentration, HR, NH, ARCC, or protein expression results compared with respective values in ZL rats without osmotic pumps.

Blood glucose concentration was significantly elevated in ZO and ZD compared with ZL rats. Although there was a trend toward decreased blood glucose concentration for all rats with ALT-711, this decrease did not reach significance, and values remained elevated compared with ZL rats (Table 2). Mean BF was decreased in ZD compared with ZL rats but increased to ZL levels after ALT-711 treatment (Fig. 1). ALT-711 also increased BF in ZO rats. ALT-711 treatment reduced distal vascular resistance in ZD rats (Fig. 1).

Representative histological sections from the middle of the stented region in ZL, ZO, and ZD rats are shown in Fig. 2. H and E staining revealed elevated NH area for ZO rats. ALT-711 treatment reduced NH area in ZL and ZO rats. A decrease in NH intrastrut thickness as a function of local radius was found in all groups with ALT-711 treatment. In-stent WSS was low for ZD compared with ZL rats (Table 3). There were no differences in in-stent WSS after ALT-711 treatment.

ARCC and protein expression results from the vessels studied are shown in Fig. 3 and summarized in Table 4. No changes were found in ARCC in the carotid arteries, thoracic aorta, or AAo. However, ARCC was significantly increased in iliac and femoral arteries of ZO and ZD rats. Increases in ARCC were also present in the arterioles of ZD rats, but these were reduced with ALT-711 treatment. There was also a reduction in ARCC in the arterioles of ZL and ZO rats that received ALT-711 treatment. AGE expression was increased in the carotid arteries, AAo, and iliac and femoral arteries of ZD rats, but this change was alleviated after ALT-711 treatment with the exception of the AAo. ALT-711 treatment was also associated with a significant decrease in AGE expression within the thoracic aorta and iliac and femoral arteries of ZO and ZD rats. Increased RAGE expression was found in the carotid arteries, iliac and femoral arteries, and arterioles of ZD rats and was unchanged by ALT-711 treatment. In contrast, RAGE expression was increased in the thoracic and abdominal regions of ZD rats receiving ALT-711 and decreased in the arterioles for ZL and ZO rats receiving ALT-711. TGF-β expression was in-

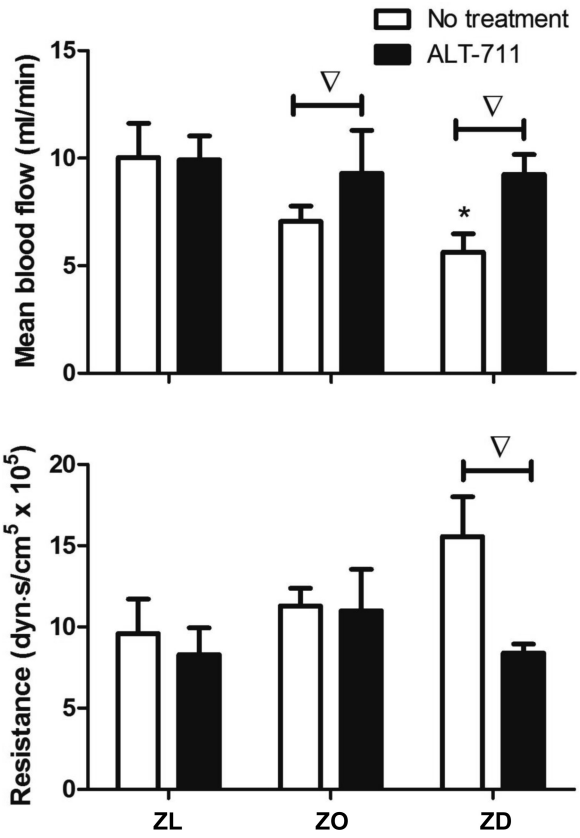

Fig. 1. Mean blood flow and resistance in Zucker lean (ZL), obese (ZO), and diabetic (ZD) rats in the absence or presence of ALT-711 treatment ($n = 6$/group). *Significantly different from ZL, ▽significant difference within group.

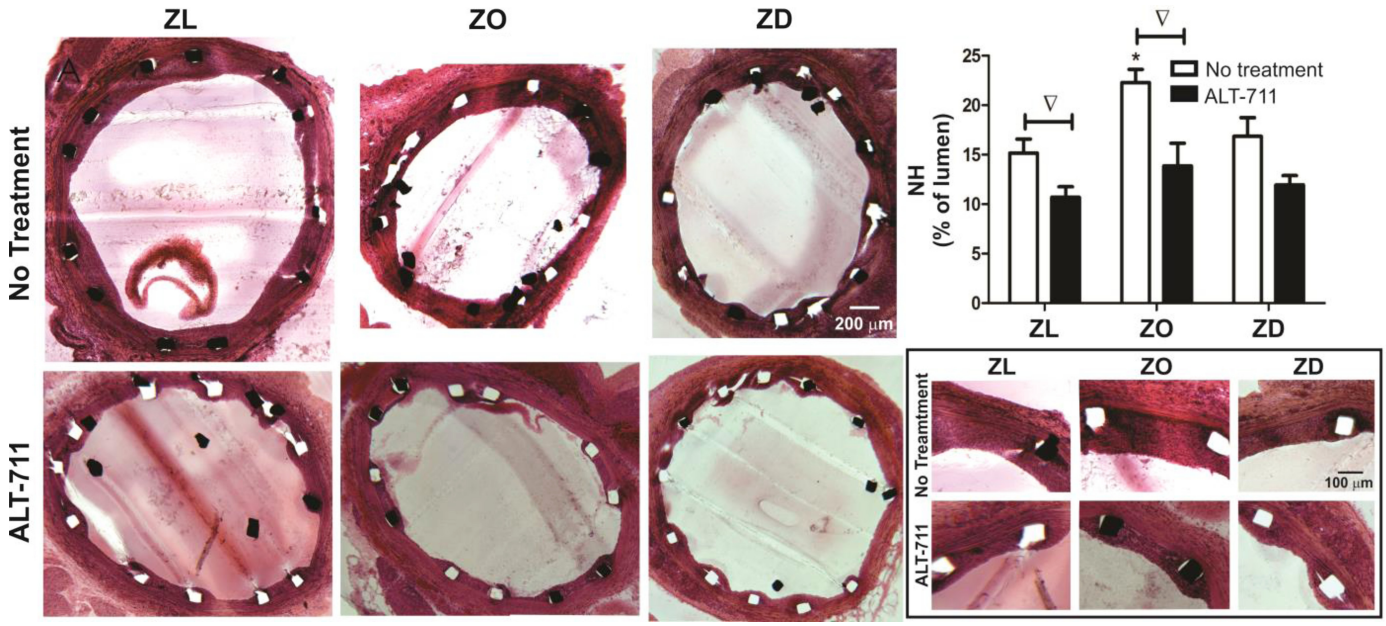

Fig. 2. Representative photomicrographs of 5-μm aortic sections from the center of the stented region stained with hematoxylin and eosin (*left*). Histograms depicting the percentage of the luminal area bounded by the stent (*top*, *right*) containing neointimal hyperplasia (NH) for ZL, ZO, and ZD rats (n = 6/group). Locally magnified photomicrographs of aortic sections showing intrastrut neointimal thickness (within inset at *bottom*, *right*) are shown. *Significantly different from ZL, ▽significant difference within group.

creased in the thoracic aorta and iliac and femoral arteries for ZD rats and was not statistically altered by treatment with ALT-711. A significant increase in TGF-β expression was also found in the AAo of ZL rats treated with ALT-711.

To further query the mechanisms associated with results obtained from the in vivo model, in vitro cell culture experiments were conducted under static and shear conditions. RAGE expression was previously shown to increase under conditions of low magnitude and reversing WSS and to affect inflammatory responses in endothelium (13). Given the enhanced RAGE expression within the AAo of ZD (Fig. 3), which was coincident with a decrease in WSS, we measured its expression as a function of WSS and matrix composition (rat type and with or without ALT) to determine the extent to which endothelial-mediated RAGE expression contributed to enhanced NH. Figure 4 shows that RAGE expression was unaffected by WSS over a range chosen to model the intrastrut region for ZL and ZD. In contrast, there was a significant increase in RAGE expression under WSS in the ZO case, which was mitigated by ALT-711.

The proliferation of SMC, the main contributor to NH after BMS implantation, was quantified in static culture (Fig. 5*A*). There was a statistically significant increase in SMC number for cells cultured on matrix from ZO compared with ZL and ZD rats, but this increase was mitigated when rats received ALT-711 before harvest. Although there were no differences between groups for EC proliferation in static culture without treatment, EC proliferation was increased for all groups receiving ALT-711, particularly when seeded on matrix from the AAo of ZO and ZD rats (Fig. 5*B*).

Table 3. *In-stent WSS from ZL, ZO, and ZD stented rats*

	ZL	ZO	ZD
No treatment	22.0 ± 1.5	12.8 ± 1.5	9.72 ± 3.7*
ALT-711	18.0 ± 2.2	17.8 ± 2.8	17.5 ± 1.4†

Values are means ± SE in dyn/cm^2; n = 3/group; *significantly different from ZL, †significant difference within group. WSS, wall shear stress.

The similarity in patterns between SMC proliferation in vitro and NH after stenting in vivo, together with the apparent influence of ALT-711 on EC proliferation independent of RAGE-mediated shearing mechanisms, prompted analysis of AGEs and RAGE expression by Western blotting. There was a statistically significant increase in AGE expression for EC seeded on matrix from ZD vs. ZL rats that was not abolished by ALT-711 (Fig. 6*A*). A reduction in RAGE expression with ALT-711 was only seen in EC on matrix from ZL rats (Fig. 6*B*). AGEs also signal through RAGE-independent pathways, including lectin-type oxidized LDL receptor 1 (LOX-1). LOX-1 expression was therefore also quantified by Western blotting to determine whether there may be differences in the route of expression for each group and in the absence or presence of ALT-711. The results show increased LOX-1 expression for ZO and ZD compared with control rats. ALT-711 increases LOX-1 expression for all groups, with this increase reaching significance for the ZL and ZD groups (Fig. 6*C*).

DISCUSSION

The objective of this investigation was to test the hypothesis that ARCC leads to increased DVR and altered hemodynamics in the stented region, promoting enhanced NH after BMS implantation in T2DM. We further proposed that that decreasing ARCC with ALT-711 would mitigate this response. There were several important findings that indicate complex interrelationships between biomechanical and biological processes governing the development of NH in obesity and diabetes. *1*) AGEs were located in nearly all vascular locations of ZD rats,

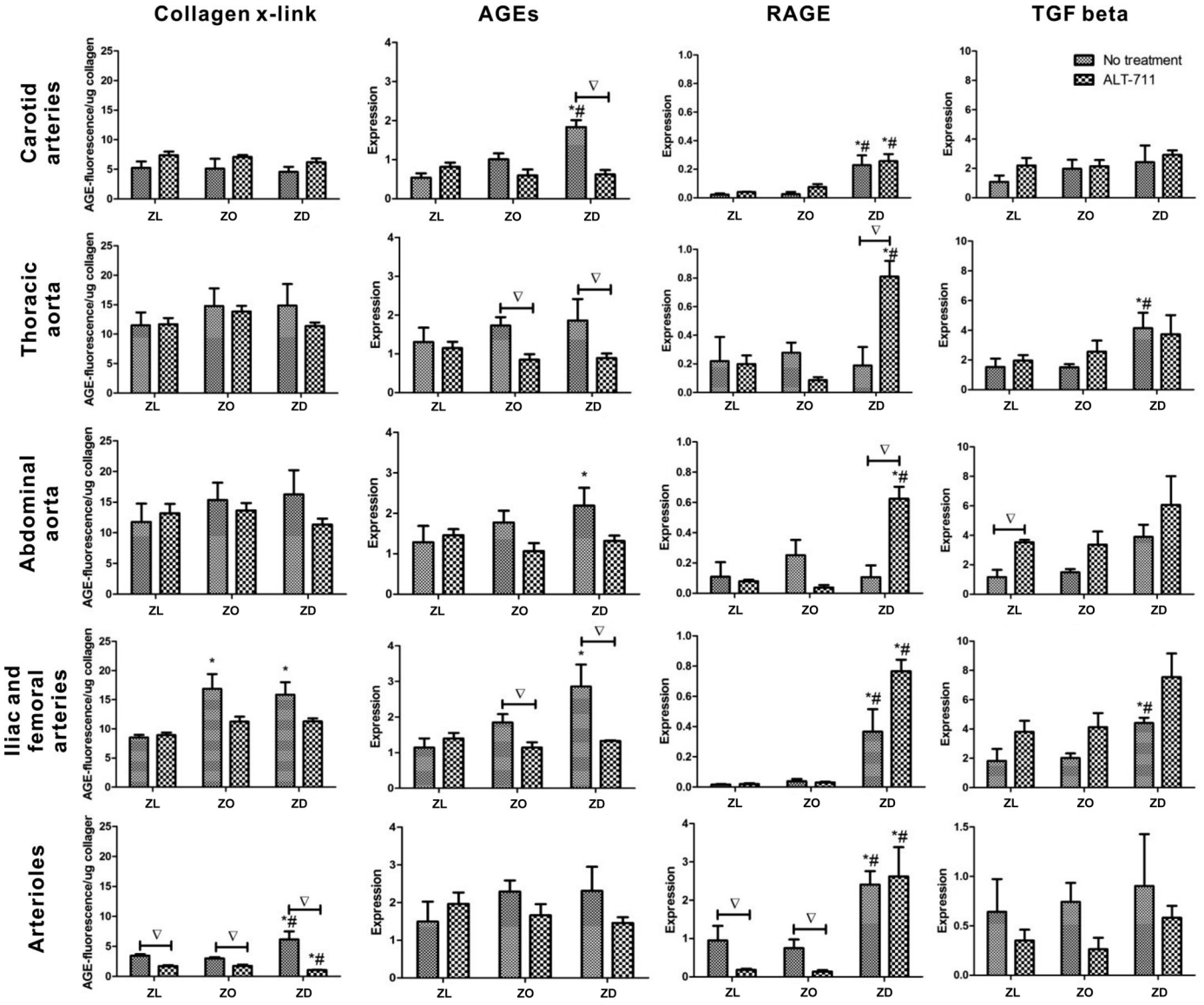

Fig. 3. Advanced glycation end-product (AGE)-related collagen cross-linking as well as transforming growth factor-β (TGF-β) and receptor for AGE (RAGE) protein expression results from the vessels studied (n = 6/group). *Significantly different from ZL, #significantly different from ZO rats, ▽significant difference within group.

confirming their elevated presence in T2DM; *2*) increasing stiffness, as indicated by ARCC, was localized to the arterioles of ZD rats but alleviated by treatment with ALT-711; *3*) mean BF decreased in ZD rats, concomitantly with increases in arteriolar resistance; *4*) WSS within the stented region was low in untreated ZD rats but comparable to ZL with ALT-711 treatment; *5*) NH within the stented region was increased in ZO but not ZD rats, but treatment reduced NH in all groups; *6*) LOX-1, but not TGF-β or RAGE, expression was elevated by ALT-711, illustrating that different AGE-mediated pathways may mediate the local NH response. These findings are discussed in more detail below.

Table 4. *Summary of AGE-related collagen cross-linking and protein expression for vessels in group of rats*

	Carotid Arteries		Thoracic Aorta		Abdominal Aorta		Iliac and Femoral Arteries		Arterioles	
Changes vs. ZL	ZO	ZD	ZO	ZD	ZO	ZD	ZO	ZD	ZO	ZD
Collagen cross-linking	NC	NC	NC	NC	NC	NC	↑	↑	NC	\↑
AGEs	NC	\↑	NC	NC	NC	↑	NC	\↑	NC	NC
RAGE	NC	↑	NC	NC	NC	NC	NC	↑	NC	↑
TGF-β	NC	NC	NC	↑	NC	NC	NC	↑	NC	NC

N = 6; NC, no change; ↑, significant increase; \, increase alleviated by ALT-711.

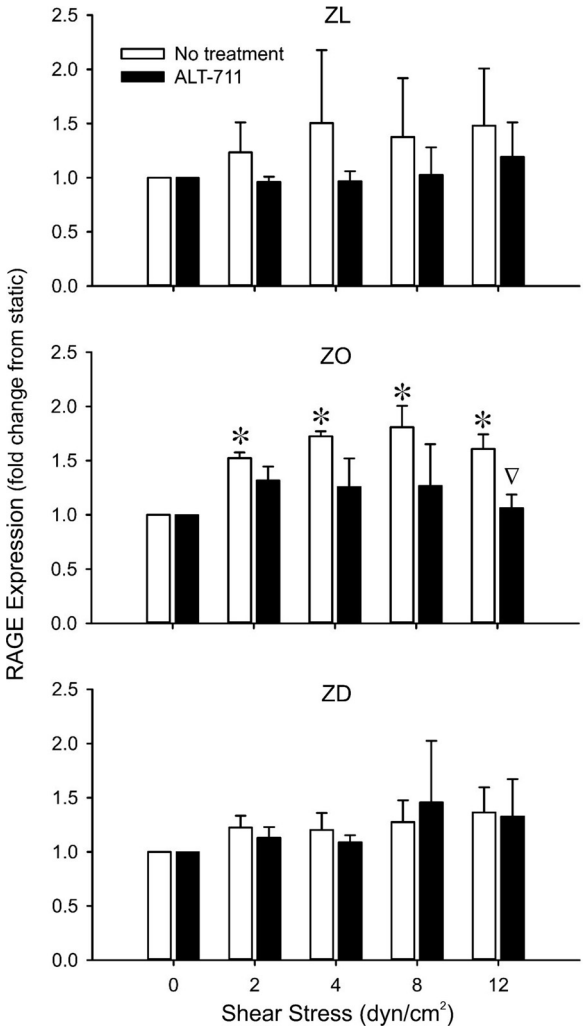

Fig. 4. Cell-shearing results of RAGE expression in response to a linearly decreasing wall shear stress (WSS) profile within a Hele-Shaw microfluidic flow chamber. The flow rate was chosen to deliver WSS magnitudes within a range of values experienced in the intrastrut region of an implanted stent within a single experiment. Endothelial cells (ECs) were seeded on decellularized matrices derived from the abdominal aorta (AAo) of ZD, ZL, and ZO rats with or without ALT-711 (20 μg/ml). Collagen I-coated (100 μg/ml) tissue culture substrates were used as a control (data not shown). *Significantly different from 0 dyn/cm², ▽significant difference within group.

Formation of ARCC occurs more rapidly during diabetic conditions (38, 49). Therefore, it is reasonable to propose that associated changes in vascular stiffness reported here alter the mechanical properties of vasculature, including the local and distal resistances to adversely influence NH after stenting. For example, AGE-induced remodeling and elevated DVR may lead to pronounced increases in wall tension, vascular damage during stenting, and localized reductions in WSS, while decreasing strain, all of which are associated with NH (5, 31). The current results suggest that increased AGE expression in the arterioles of ZD rats appears to decrease BF by increasing downstream vascular stiffness and hence resistance. Increased ARCC within the arterioles of ZD rats was absent after ALT-711 treatment, suggesting that this cross-link antagonist preferentially reduces AGE-induced stiffness in distal vessels. These findings are consistent with previous studies showing that ARCC is an important factor that promotes vascular stiffness. Conversely, ALT-711 reduces established AGEs and collagen cross-linking (47), decreases arterial stiffness, and enhances cardiac output (1, 16, 25). Consistent with the current results, Kass et al. (25) also found that ALT-711 could alleviate vascular dysfunction and wall stiffness without changing mean arterial BP.

There were two findings of particular interest mediated by ALT-711 within the stented region of ZD rats. There is a reduction in resistance afforded by ALT-711, which is associated with flow and WSS values that are similar to ZL (compared with untreated rats). Interestingly, the amount of NH was reduced for all rats receiving ALT-711 (ZD as well as ZO and ZL). RAGE expression was pronounced within the stented region, but in vitro WSS studies failed to show a difference when EC were cultured on matrix from ZD rats in the absence or presence of treatment. In contrast, the expression of LOX-1 was increased for cells seeded on matrix from ZO and ZD, compared with ZL, rats. This elevated expression was further pronounced when rats were treated with ALT-711 before the harvesting of arterial tissue. The proliferation of SMC, a primary contributor to NH after BMS implantation, showed trends similar to NH results seen after AAo stenting. ZO results were most pronounced and significantly different from ZL and ZD but alleviated by treatment. We interpret these collective results as evidence that changes in hemodynamics in the stented region are secondary to vascular changes induced by factors associated with the metabolic dysregulation of diabetes, including enhanced AGE expression and ARCC studied here.

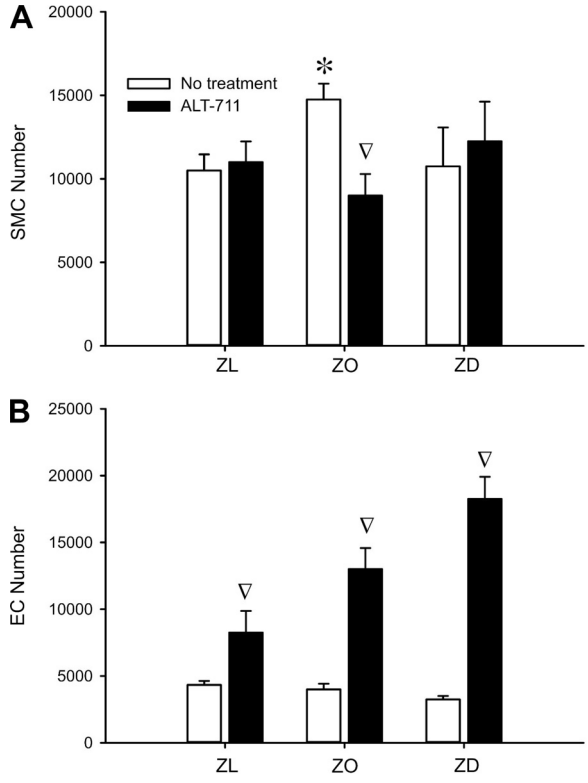

Fig. 5. Static cell culture results of smooth muscle cell (SMC) (*A*) and EC (*B*) proliferation. All results are from the respective cell type seeded on matrix from the AAo of ZD, ZL, and ZO rats with or without ALT-711. *Significantly different from ZL, ▽significant difference within group.

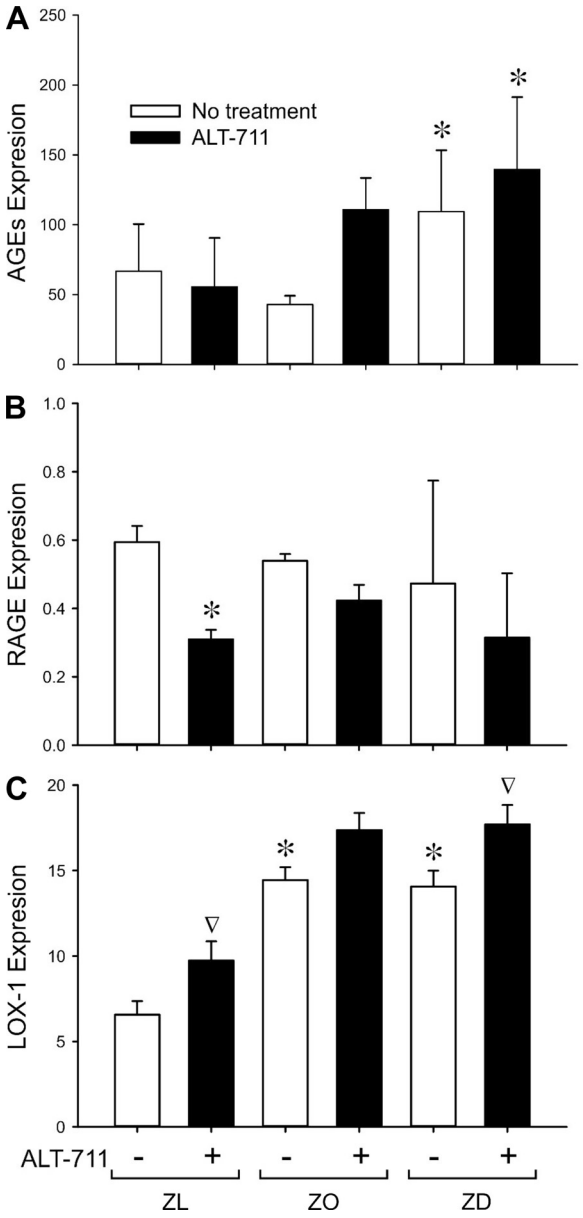

Fig. 6. Static cell culture results of AGEs (*A*), RAGE (*B*), and lectin-type oxidized LDL receptor 1 (LOX-1) (*C*) expression from Western blot of ECs. Results are expressed as a ratio of expression to loading control. All results are from cells seeded on matrix from the AAo of ZD, ZL, and ZO rats with or without ALT-711. *Significantly different from ZL, ▽significant difference within group.

It is likely that biomechanical and biological factors act synergistically at some level to affect mechanisms that contribute to NH, but the relative contribution of each requires additional research.

Although local changes in stiffness mentioned above may influence diameter and the response of an artery to stent-induced injury, low WSS within the stent can also influence NH through endothelial-mediated mechanotransduction via several signaling pathways (28, 55). To our knowledge, this is the first investigation comparing WSS between lean, obese, and T2DM rats. Our results demonstrate that WSS from the stented region was reduced for ZD compared with ZL rats. This finding occurs from reductions in BF and hence lower velocity and WSS, concomitant with higher downstream vascular resistance. Enhanced NH in the current study was apparently not mediated by shear modulation of RAGE expression. Interestingly, NH was highest in ZO compared with ZD and ZL rats. Jonas et al. (24) similarly observed elevated NH in ZO compared with ZL and ZD rats, and other studies also found severely hyperglycemic animals to have NH equal to or even decreased relative to controls (23, 37). Thus the interplay between biomechanical and molecular mechanisms contributing to NH under obesity and diabetes is complex. Additional studies will be needed to demonstrate causality in linking the changes in WSS to enhanced NH.

RAGE is an important receptor for AGEs, which was previously shown to be regulated by WSS in endothelial cells (13). AGE signaling is associated with endothelial dysfunction. Specifically, the interaction of AGEs and RAGE activate endothelial adhesion molecules like VCAM-1, NF-κB, protein kinase C, ERK, and TGF-β (9, 30, 52), which accelerate atherosclerosis by enhancing monocyte adhesion and vascular permeability. AGE expression was increased in the carotid arteries, AAo, and iliac and femoral arteries of ZD rats in the current investigation. These changes were alleviated by ALT-711, consistent with evidence showing that ALT-711 can reduce AGE accumulation and attenuate atherosclerosis (16). In contrast, RAGE expression was increased in ZD rats with or without ALT-711. Previous studies showed that ALT-711 decreased RAGE protein expression (6, 16). However, these studies were not tested in the stented diabetic condition, and a higher dose of ALT-711 was used. The lack of differences in RAGE expression within the shearing experiments could be attributable to experimental variability and insufficient replication, but they may also further implicate the involvement of different pathways in the pathological response. It is also possible that enhanced accessibility to AGEs and other RAGE ligands in the obese or diabetic animals or other factors like posttranslational modifications of RAGE (42) are more important to the outcome than its expression. Moreover, although ALT-711 reverses ARCC (8), it may not directly alter RAGE expression. RAGE can be expressed, not only through AGEs, but also by the S100/calgranulin family of proinflammatory molecules, high-mobility group box-1, β-sheet fibrils, amyloid-β peptide, and the β2-integrin Mac-1 (41). These findings suggest that isolated modification of AGE expression after treatment by ALT-711 man not modulate all pathways that can lead to RAGE expression. For example, Watson et al. (51) also reported that ALT-711 decreased AGEs in a diabetic mouse model with genetic deletion of RAGE (knockout).

AGEs can also signal through RAGE-independent pathways. Of note, our results show increased LOX-1 expression for ZO and ZD compared with control rats and that ALT-711 increases LOX-1 expression for all groups. Although the role of LOX-1 has previously been described following balloon arterial injury in rats (21, 54), the ability of ALT-711 to influence AGEs through LOX-1, particularly with application to the inherent injury caused by stenting, had not yet been shown. Our observations of altered LOX-1 expression on decellularized matrices do not allow us to discern the relative importance of altered hemodynamics vs. other structural changes to the vessel wall in contributing to enhanced NH in ZO or ZD rats.

We found that TGF-β expression was not influenced by treatment with ALT-711, which is inconsistent with previous studies showing increased TGF-β protein expression in regions adjacent to stent struts as early as 5 days after stenting (34, 50). TGF-β promotes extracellular matrix production and cellular proliferation as evidenced by enhanced NH when the TGF-β gene was transferred into normal porcine arteries (33). Our results pointing to the importance of extracellular matrix in the NH response may have differed from this prior investigation because we sampled tissue adjacent but not within the stented region. The stented region of rats in the current investigation was used for WSS calculation or quantification of NH.

The current static cell culture results indicate EC proliferation increases with ALT-711, particularly in the ZO and ZD cases. These results suggest that, in addition to the ability to prevent ARCC, ALT-711 may have a beneficial effect on re-endothelialization, which could have important ramifications for reducing the likelihood of late stent thrombosis. The functionality of these ECs and whether ALT-711 has a similar impact in the setting of the various drug-eluting stent agents (e.g., everolimus, paclitaxel, and zotarolimus) remain to be determined in future experiments conducted through follow-up studies.

The current results should be interpreted relative to the methods applied. BP was measured using a fluid-filled catheter placed in the carotid artery, but the flow transducer was positioned just above the stented region for measurement of flow into the stented region. There is a distance between these two measurement locations, so the relationship between BP, flow, and resistance calculated may not account for the portion of flow distributed to the liver and organs in the abdomen. The alternative approach of obtaining all measurements in the same position would require a fluid-filled needle positioned above the stented region for BP measurement, which is technically challenging and would add to potential complications for the current experimental protocol. In addition, the stent was deployed below the renal vascular region so as to not disturb the kidneys, which can also influence flow and resulting BP. Differences in body weight would be expected for ZO and ZD vs. ZL rats. The age of rats used here might have precluded this occurrence, which is expected to result in inflammation and likely further exacerbate the neointimal response after stenting.

In summary, the results demonstrated that the cross-linking antagonist, ALT-711, decreased ARCC and arteriolar stiffness in obese and diabetic rats after stent implantation. ALT-711 decreased DVR, increased local BF, and led to consistent values of WSS within the stented region, suggesting that AGE-induced vascular remodeling can alter in-stent hemodynamics. This is predicted to play an important role in NH formation although the underlying mechanisms require further study, particularly in the context of the complex milieu of diabetes. The finding that ALT-711 treatment reduced NH in lean, obese, and diabetic rats through RAGE-independent pathways, while simultaneously promoting endothelial proliferation, suggests that this agent may be effective to decrease stent restenosis regardless of patient glycemic status.

ACKNOWLEDGMENTS

The authors thank John Tessmer and David Schwabe (Department of Anesthesiology, Medical College of Wisconsin) for technical assistance with the experimental protocol, as well as Thomas J. Eddinger, PhD (Department of Biological Sciences, Marquette University) and Laura M. Ellwein, PhD (Department of Mathematics and Applied Mathematics, Virginia Commonwealth University) for scientific contributions during the early stages of this investigation.

GRANTS

This work was supported by a Junior Faculty Award from the American Diabetes Foundation (7-08-JF-25 to J. LaDisa).

DISCLOSURES

No conflicts of interest, financial or otherwise, are declared by the authors.

AUTHOR CONTRIBUTIONS

Author contributions: H.W., D.W., J.R.K., A.G.P., and J.F.L. conception and design of research; H.W., D.W., A.G.P., A.R., and J.F.L. performed experiments; H.W., D.W., J.R.K., J.M.T., A.G.P., A.R., S.S., and J.F.L. analyzed data; H.W., D.W., J.R.K., J.M.T., A.G.P., S.S., and J.F.L. interpreted results of experiments; H.W., D.W., J.M.T., A.G.P., and J.F.L. prepared figures; H.W., J.R.K., and J.F.L. drafted manuscript; H.W., D.W., J.R.K., J.M.T., A.G.P., S.S., and J.F.L. edited and revised manuscript; H.W., D.W., J.R.K., J.M.T., A.G.P., A.R., S.S., and J.F.L. approved final version of manuscript.

REFERENCES

1. **Asif M, Egan J, Vasan S, Jyothirmayi GN, Masurekar MR, Lopez S, Williams C, Torres RL, Wagle D, Ulrich P, Cerami A, Brines M, Regan TJ.** An advanced glycation endproduct cross-link breaker can reverse age-related increases in myocardial stiffness. *Proc Natl Acad Sci USA* 97: 2809–2813, 2000.
2. **Bakris GL, Bank AJ, Kass DA, Neutel JM, Preston RA, Oparil S.** Advanced glycation end-product cross-link breakers. A novel approach to cardiovascular pathologies related to the aging process. *Am J Hypertens* 17: 23S–30S, 2004.
3. **Berry C, Tardif JC, Bourassa MG.** Coronary heart disease in patients with diabetes. II: Recent advances in coronary revascularization. *J Am Coll Cardiol* 49: 643–656, 2007.
4. **Bradford MM.** A rapid and sensitive method for the quantitation of microgram quantities of protein utilizing the principle of protein-dye binding. *Anal Biochem* 72: 248–254, 1976.
5. **Brownlee M.** Advanced protein glycosylation in diabetes and aging. *Annu Rev Med* 46: 223–234, 1995.
6. **Candido R, Forbes JM, Thomas MC, Thallas V, Dean RG, Burns WC, Tikellis C, Ritchie RH, Twigg SM, Cooper ME, Burrell LM.** A breaker of advanced glycation end products attenuates diabetes-induced myocardial structural changes. *Circ Res* 92: 785–792, 2003.
7. **Center for Disease Control and Prevention.** *National Diabetes Fact Sheet: General Information and National Estimates on Diabetes in the United States*. Atlanta, GA: National Center for Chronic Disease Prevention and Health Promotion, 2011.
8. **Cooper ME.** Importance of advanced glycation end products in diabetes-associated cardiovascular and renal disease. *Am J Hypertens* 17: 31S–38S, 2004.
9. **Cortizo AM, Lettieri MG, Barrio DA, Mercer N, Etcheverry SB, McCarthy AD.** Advanced glycation end-products (AGEs) induce concerted changes in the osteoblastic expression of their receptor RAGE and in the activation of extracellular signal-regulated kinases (ERK). *Mol Cell Biochem* 250: 1–10, 2003.
10. **Coughlan MT, Forbes JM, Cooper ME.** Role of the AGE crosslink breaker, alagebrium, as a renoprotective agent in diabetes. *Kidney Int Suppl* 106: S54–S60, 2007.
11. **De la Torre Hernandez JM, Alfonso F, Sanchez Recalde A, Jimenez Navarro MF, Perez de Prado A, Hernandez F, Abdul-Jawad Altisent O, Roura G, Garcia Camarero T, Elizaga J, Rivero F, Gimeno F, Calviño R, Moreu J, Bosa F, Rumoroso JR, Bullones JA, Gallardo A, Fernandez Diaz JA, Ruiz Arroyo JR, Aragon V, Masotti M; ESTROFA-LM Study Group.** Comparison of paclitaxel-eluting stents (Taxus) and everolimus-eluting stents (Xience) in left main coronary artery disease with 3 years follow-up (from the ESTROFA-LM registry). *Am J Cardiol* 111: 676–683, 2013.

12. **Deuse T, Ikeno F, Robbins RC, Schrepfer S.** Imaging in-stent restenosis: an inexpensive, reliable, and rapid preclinical model. *J Vis Exp* 14: 1346, 2009.
13. **DeVerse JS, Bailey KA, Jackson KN, Passerini AG.** Shear stress modulates RAGE-mediated inflammation in a model of diabetes-induced metabolic stress. *Am J Physiol Heart Circ Physiol* 302: H2498–H2508, 2012.
14. **DeVerse JS, Sandhu AS, Mendoza N, Edwards CM, Sun C, Simon SI, Passerini AG.** Shear stress modulates VCAM-1 expression in response to TNF-α and dietary lipids via interferon regulatory factor-1 in cultured endothelium. *Am J Physiol Heart Circ Physiol* 305: H1149–H1157, 2013.
15. **Dudek D, Legutko J, Heba G, Bartus S, Partyka L, Huk I, Dembinska-Kiec A, Kaluza GL, Dubiel JS.** L-Arginine supplementation does not inhibit neointimal formation after coronary stenting in human beings: an intravascular ultrasound study. *Am Heart J* 147: E12, 2004.
16. **Forbes JM, Yee LT, Thallas V, Lassila M, Candido R, Jandeleit-Dahm KA, Thomas MC, Burns WC, Deemer EK, Thorpe SR, Cooper ME, Allen TJ.** Advanced glycation end product interventions reduce diabetes-accelerated atherosclerosis. *Diabetes* 53: 1813–1823, 2004.
17. **Garasic JM, Edelman ER, Squire JC, Seifert P, Williams MS, Rogers C.** Stent and artery geometry determine intimal thickening independent of arterial injury. *Circulation* 101: 812–818, 2000.
18. **Gilbert J, Raboud J, Zinman B.** Meta-analysis of the effect of diabetes on restenosis rates among patients receiving coronary angioplasty stenting. *Diabetes Care* 27: 990–994, 2004.
19. **Goldfine AB, Beckman JA.** Life and death in Denmark: lessons about diabetes and coronary heart disease. *Circulation* 117: 1914–1917, 2008.
20. **Hakim DA, Mintz GS, Sanidas E, Rusinova R, Weisz G, Leon MB, Moses JW, Stone GW, Maehara A.** Serial gray scale intravascular ultrasound findings in late drug-eluting stent restenosis. *Am J Cardiol* 111: 695–699, 2013.
21. **Hinagata J, Kakutani M, Fujii T, Naruko T, Inoue N, Fujita Y, Mehta JL, Ueda M, Sawamura T.** Oxidized LDL receptor LOX-1 is involved in neointimal hyperplasia after balloon arterial injury in a rat model. *Cardiovasc Res* 69: 263–271, 2006.
22. **Hioki H, Kumazaki S, Izawa A.** Critical in-stent restenosis following fracture of biolimus-eluting stent: a report of 2 cases. *J Invasive Cardiol* 25: E11–E13, 2013.
23. **Indolfi C, Torella D, Cavuto L, Davalli AM, Coppola C, Esposito G, Carriero MV, Rapacciuolo A, Di Lorenzo E, Stabile E, Perrino C, Chieffo A, Pardo F, Chiariello M.** Effects of balloon injury on neointimal hyperplasia in streptozotocin-induced diabetes and in hyperinsulinemic nondiabetic pancreatic islet-transplanted rats. *Circulation* 103: 2980–2986, 2001.
24. **Jonas M, Edelman ER, Groothuis A, Baker AB, Seifert P, Rogers C.** Vascular neointimal formation and signaling pathway activation in response to stent injury in insulin-resistant and diabetic animals. *Circ Res* 97: 725–733, 2005.
25. **Kass DA, Shapiro EP, Kawaguchi M, Capriotti AR, Scuteri A, deGroof RC, Lakatta EG.** Improved arterial compliance by a novel advanced glycation end-product crosslink breaker. *Circulation* 104: 1464–1470, 2001.
26. **Khan W, Farah S, Domb AJ.** Drug eluting stents: developments and current status. *J Control Release* 161: 703–712, 2012.
27. **Kutryk MJ, Foley DP, van den Brand M, Hamburger JN, van der Giessen WJ, deFeyter PJ, Bruining N, Sabate M, Serruys PW.** Local intracoronary administration of antisense oligonucleotide against c-myc for the prevention of in-stent restenosis: results of the randomized investigation by the Thoraxcenter of antisense DNA using local delivery and IVUS after coronary stenting (ITALICS) trial. *J Am Coll Cardiol* 39: 281–287, 2002.
28. **LaDisa JF Jr, Olson LE, Hettrick DA, Warltier DC, Kersten JR, Pagel PS.** Axial stent strut angle influences wall shear stress after stent implantation: analysis using 3D computational fluid dynamics models of stent foreshortening. *Biomed Eng Online* 4: 59, 2005.
29. **LaDisa JF Jr, Olson LE, Molthen RC, Hettrick DA, Pratt PF, Hardel MD, Kersten JR, Warltier DC, Pagel PS.** Alterations in wall shear stress predict sites of neointimal hyperplasia after stent implantation in rabbit iliac arteries. *Am J Physiol Heart Circ Physiol* 288: H2465–H2475, 2005.
30. **Meerwaldt R, Links T, Zeebregts C, Tio R, Hillebrands JL, Smit A.** The clinical relevance of assessing advanced glycation endproducts accumulation in diabetes. *Cardiovasc Diabetol* 7: 29, 2008.
31. **Morrison TM, Choi G, Zarins CK, Taylor CA.** Circumferential and longitudinal cyclic strain of the human thoracic aorta: age-related changes. *J Vasc Surg* 49: 1029–1036, 2009.
32. **Moses JW, Leon MB, Popma JJ, Fitzgerald PJ, Holmes DR, O'Shaughnessy C, Caputo RP, Kereiakes DJ, Williams DO, Teirstein PS, Jaeger JL, Kuntz RE.** Sirolimus-eluting stents versus standard stents in patients with stenosis in a native coronary artery. *N Engl J Med* 349: 1315–1323, 2003.
33. **Nabel EG, Shum L, Pompili VJ, Yang ZY, San H, Shu HB, Liptay S, Gold L, Gordon D, Derynck R, Nabel GJ.** Direct transfer of transforming growth factor beta 1 gene into arteries stimulates fibrocellular hyperplasia. *Proc Natl Acad Sci USA* 90: 10759–10763, 1993.
34. **Nikol S, Isner JM, Pickering JG, Kearney M, Leclerc G, Weir L.** Expression of transforming growth factor-beta 1 is increased in human vascular restenosis lesions. *J Clin Invest* 90: 1582–1592, 1992.
35. **Noh H, King GL.** The role of protein kinase C activation in diabetic nephropathy. *Kidney Int Suppl* S49–S53, 2007.
36. **Oyamada S, Ma X, Wu T, Robich MP, Wu H, Wang X, Buchholz B, McCarthy S, Bianchi CF, Sellke FW, Laham R.** Trans-iliac rat aorta stenting: a novel high throughput preclinical stent model for restenosis and thrombosis. *J Surg Res* 166: e91–e95, 2011.
37. **Park SH, Marso SP, Zhou Z, Foroudi F, Topol EJ, Lincoff AM.** Neointimal hyperplasia after arterial injury is increased in a rat model of non-insulin-dependent diabetes mellitus. *Circulation* 104: 815–819, 2001.
38. **Peppa M, Uribarri J, Vlassara H.** The role of advanced glycation end products in the development of atherosclerosis. *Curr Diab Rep* 4: 31–36, 2004.
39. **Peppa M, Vlassara H.** Advanced glycation end products and diabetic complications: a general overview. *Hormones (Athens)* 4: 28–37, 2005.
40. **Ryan J, Cohen DJ.** Are drug-eluting stents cost-effective? It depends on whom you ask. *Circulation* 114: 1736–1743, 2006.
41. **Schmidt AM, Yan SD, Yan SF, Stern DM.** The biology of the receptor for advanced glycation end products and its ligands. *Biochim Biophys Acta* 1498: 99–111, 2000.
42. **Srikrishna G, Huttunen HJ, Johansson L, Weigle B, Yamaguchi Y, Rauvala H, Freeze HH.** *N*-glycans on the receptor for advanced glycation end products influence amphoterin binding and neurite outgrowth. *J Neurochem* 80: 998–1008, 2002.
43. **Stefek M, Gajdosik A, Gajdosikova A, Krizanova L.** p-Dimethylaminobenzaldehyde-reactive substances in tail tendon collagen of streptozotocin-diabetic rats: temporal relation to biomechanical properties and advanced glycation endproduct (AGE)-related fluorescence. *Biochim Biophys Acta* 1502: 398–404, 2000.
44. **Stone GW, Kedhi E, Kereiakes DJ, Parise H, Fahy M, Serruys PW, Smits PC.** Differential clinical responses to everolimus-eluting and Paclitaxel-eluting coronary stents in patients with and without diabetes mellitus. *Circulation* 124: 893–900, 2011.
45. **Tas¸kiran DT, Tas¸kiran E, Yercan H, Kutay FZ.** Quantification total collagen in rabbit tendon by the Sirius red. *Tr J Med Sci* 29: 7–9, 1999.
46. **Tsou JK, Gower RM, Ting HJ, Schaff UY, Insana MF, Passerini AG, Simon SI.** Spatial regulation of inflammation by human aortic endothelial cells in a linear gradient of shear stress. *Microcirculation* 15: 311–323, 2008.
47. **Vasan S, Zhang X, Kapurniotu A, Bernhagen J, Teichberg S, Basgen J, Wagle D, Shih D, Terlecky I, Bucala R, Cerami A, Egan J, Ulrich P.** An agent cleaving glucose-derived protein crosslinks in vitro and in vivo. *Nature* 382: 275–278, 1996.
48. **Vladic N, Ge ZD, Leucker T, Brzezinska AK, Du JH, Shi Y, Warltier DC, Pratt PF Jr, Kersten JR.** Decreased tetrahydrobiopterin and disrupted association of Hsp90 with eNOS by hyperglycemia impair myocardial ischemic preconditioning. *Am J Physiol Heart Circ Physiol* 301: H2130–H2139, 2011.
49. **Vlassara H, Palace MR.** Diabetes and advanced glycation endproducts. *J Intern Med* 251: 87–101, 2002.
50. **Ward MR, Agrotis A, Kanellakis P, Hall J, Jennings G, Bobik A.** Tranilast prevents activation of transforming growth factor-beta system, leukocyte accumulation, and neointimal growth in porcine coronary arteries after stenting. *Arterioscler Thromb Vasc Biol* 22: 940–948, 2002.
51. **Watson AM, Gray SP, Jiaze L, Soro-Paavonen A, Wong B, Cooper ME, Bierhaus A, Pickering R, Tikellis C, Tsorotes D, Thomas MC, Jandeleit-Dahm KA.** Alagebrium reduces glomerular fibrogenesis and inflammation beyond preventing RAGE activation in diabetic apolipoprotein E knockout mice. *Diabetes* 61: 2105–2113, 2012.

52. **Wendt T, Tanji N, Guo J, Hudson BI, Bierhaus A, Ramasamy R, Arnold B, Nawroth PP, Yan SF, D'Agati V, Schmidt AM.** Glucose, glycation, and RAGE: implications for amplification of cellular dysfunction in diabetic nephropathy. *J Am Soc Nephrol* 14: 1383–1395, 2003.
53. **Windberger U, Bartholovitsch A, Plasenzotti R, Korak KJ, Heinze G.** Whole blood viscosity, plasma viscosity and erythrocyte aggregation in nine mammalian species: reference values and comparison of data. *Exp Physiol* 88: 431–440, 2003.
54. **Yao EH, Fukuda N, Ueno T, Matsuda H, Matsumoto K, Nagase H, Matsumoto Y, Takasaka A, Serie K, Sugiyama H, Sawamura T.** Novel gene silencer pyrrole-imidazole polyamide targeting lectin-like oxidized low-density lipoprotein receptor-1 attenuates restenosis of the artery after injury. *Hypertension* 52: 86–92, 2008.
55. **Yazdani SK, Nakano M, Otsuka F, Kolodgie FD, Virmani R.** Atheroma and coronary bifurcations: before and after stenting. *EuroIntervention* 6, *Suppl J*: J24–J30, 2010.